

Spectral denoising for unsupervised analysis of correlated ionic transport

Nicola Molinari,* Yu Xie, and Ian Leifer

*John A. Paulson School of Engineering and Applied Sciences,
Harvard University, Cambridge, MA 02138, USA.*

Mordechai Kornbluth

*Robert Bosch LLC, Research and Technology Center,
Cambridge, Massachusetts 02142, USA*

Boris Kozinsky†

*John A. Paulson School of Engineering and Applied Sciences,
Harvard University, Cambridge, MA 02138, USA. and
Robert Bosch LLC, Research and Technology Center,
Cambridge, Massachusetts 02142, USA*

(Dated: August 18, 2022)

Computation of correlated ionic transport properties from molecular dynamics in the Green-Kubo formalism is expensive as one cannot rely on the affordable mean square displacement approach. We use spectral decomposition of the short-time ionic displacement covariance to learn a set of diffusion eigenmodes that encode the correlation structure and form a basis for analyzing the ionic trajectories. This allows to systematically reduce the uncertainty and accelerate computations of ionic conductivity in systems with a steady-state correlation structure. We provide mathematical and numerical proofs of the method’s robustness, and demonstrate it on realistic electrolyte materials.

I. INTRODUCTION

Understanding the transport of ionic species is of central importance in a variety of fields ranging from physics and biophysics[1, 2] to chemistry in general[3]. Of particular relevance for energy storage solutions, the design of next-generation metal-ion batteries depends on the development of fast ion-conducting and stable electrolyte materials[4–6].

As the total ionic conductivity is proportional to the number of charge carriers, high concentrations of ions are typically targeted. Consequently, due to both high concentrations and long-range Coulomb interactions, the correlation between ions becomes non-negligible[7, 8]. The physics of ion correlations and effects on transport properties are complex as they can be either beneficial[9, 10] or detrimental[11, 12] depending on the composition and concentrations. To capture correlation effects in transport of concentrated solutions, it is necessary to collect statistics of the total ionic flux fluctuations [13, 14]. This method, based on the exact Green Kubo linear response formalism at equilibrium, yields only a single total flux value for the entire atomic configuration. As a result, to reach sufficient convergence of the statistics, long simulations are typically needed, especially for large systems where flux fluctuations are small. The total flux approach yields exact (unbiased) estimates of ionic conductivity but with a high variance that increases linearly with the system size.

These limitations often lead to the adoption of dilute-solution approximations such as the Nernst-Einstein approach, which uses individual atom means square displacement (MSD) and assumes that all atoms are uncorrelated. In this case the variance of the estimate is lower and independent of the system size, leading to fast although often incorrect (biased) estimates. Methods capable of providing accurate ionic conductivity, κ , at a reasonable computational cost are therefore extremely valuable for dealing with correlated ionic transport and for discovery and understanding of next-generation high-performance electrolytes. If the short-range correlations are strong, time-independent, and known a priori, such as bonds between atoms in a molecular liquid, with negligible inter-molecular correlations, displacements of the molecules rather than atoms can be used as the basis in the Nernst-Einstein MSD formulation. In the case of electrolytes, for example, the cluster Nernst-Einstein method treats ion clusters as uncorrelated charge-moving entities, and applies the Nernst-Einstein approach to estimate the cluster contribution to the conductivity[15]. This approach reduces the estimate uncertainty and yields correct transport properties only if the pre-defined clusters or molecules are uncorrelated and immutable, meaning that their persistence time is longer than the time needed to reach the diffusive regime. These assumptions are generally not true for a wide range of systems, such as concentrated liquid and single-ion solid-state electrolytes. Also, the structure and persistent times of atomic groups are often not known ahead of time.

In this work, we introduce a data-driven approach to learn the diffusive modes from the full interatomic displacement covariance matrix via its spectral decomposition, without prior assumptions about the range

* nmolinari@seas.harvard.edu

† bkoz@seas.harvard.edu

and structure of the correlation, other than it is time-independent. We then use the learned eigenvectors to greatly reduce the variance and accelerate the estimation of the ionic conductivity for correlated systems, with rigorous provable bounds on the bias.

II. THEORY & METHOD

In the Green-Kubo linear response theory [16] the (ionic) conductivity κ can be written in an Einstein (position) form as:

$$\kappa = \frac{F^2}{6N_A^2 V k_B \mathcal{T}} \lim_{\tau \rightarrow \infty} \frac{\partial}{\partial \tau} \sum_{ij} q_i q_j \langle \mathcal{C}_{ij}(\tau) \rangle. \quad (1)$$

Here F is the Faraday's constant, N_A the Avogadro's number, V the volume, k_B the Boltzmann's constant, \mathcal{T} the temperature, $\langle \dots \rangle$ indicates an element-by-element average (see below), and q_i is the charge and $\mathbf{r}_i(t)$ the position vector of particle i at time t . The position displacement covariance matrix is $\mathcal{C}_{ij}(\tau) = [\mathbf{r}_i(\tau+t) - \mathbf{r}_i(t)] \cdot [\mathbf{r}_j(\tau+t) - \mathbf{r}_j(t)]$ and indices i, j run over all moving charged particles.

The diagonal $i = j$ represents each particle's squared displacements, and the inter-particle displacement correlation is encoded in the off-diagonal $i \neq j$ elements. If the motions of particles i and j are uncorrelated, the averaged, off-diagonal element $\langle \mathcal{C}_{i \neq j}(\tau) \rangle \rightarrow 0$ for values of τ greater than the typical collision time scale. Consequently, the relevant information about the diffusion of an uncorrelated system lies exclusively on the diagonal of $\langle \mathcal{C}_{ij}(\tau) \rangle$. Replacing the $\langle \mathcal{C}_{i \neq j}(\tau) \rangle$ terms with zeros is equivalent to the widely-adopted Nernst-Einstein formulation to calculate the conductivity[17] from the mean square displacement, which is only correct in the infinitely dilute uncorrelated limit. In this case each diagonal value contributes independently to the variance of the conductivity estimate, which is reduced by a factor of N (number of particles) compared to the variance of the total flux estimate of the conductivity[18].

Finally, the $\langle \mathcal{C}_{ij}(\tau) \rangle$ average is obtained by performing multiple instances of the same experiment, and by implementing time-block window averaging[19]. The issue with the latter averaging is that the statistics becomes poorer for longer time-blocks: for a simulation of total time T , we can extract more time windows of delay $\tau_1 = t_1$ than $\tau_2 = t_2$, for $t_1 < t_2 < T$, and this translates in the averaging of $\langle \mathcal{C}_{ij}(\tau_1) \rangle$ and $\langle \mathcal{C}_{ij}(\tau_2) \rangle$. As a result, determination of transport properties becomes noisier, and long MD simulations are needed to obtain the total flux conductivity estimate within a reasonable uncertainty.

Our approach is based on the eigenvectors of $\langle \mathcal{C}_{ij}(\tau) \rangle$ averaged using a short time interval $\tau = \tau_1$ greater than the minimum time needed for the system to reach the diffusive regime. $\langle \mathcal{C}_{ij}(\tau_1) \rangle$ contains the most well-converged information about the correlation of the system because

any time window $\tau_n > \tau_1$ has fewer position-position correlation matrices to average over. We then use the learned spectral information to reduce the statistical variance of the estimate of κ for any time window $\tau_n > \tau_1$. The only assumption of our approach is that the correlation structure of the system under investigation does not change over time, which is generally true for non-reacting ergodic systems in thermodynamic equilibrium.

Before describing the spectral denoising approach, we introduce the terminology used throughout this work.

Total flux, or full summation (FS) is the exact Green-Kubo conductivity based on the summation over *all* i, j elements of $\langle \mathcal{C}_{ij}(\tau) \rangle$ as in Equation 1.

Nernst-Einstein mean squared displacement (MSD) approach based on the trace of $\langle \mathcal{C}_{ij}(\tau) \rangle$, assumes the cross-terms $i \neq j$ are zero.

Spectral denoising (SD) refers to the method developed in this work, where the denoised $\langle \mathcal{C}_{ij}^*(\tau) \rangle$ is used to compute conductivity, as described below.

To quantify the degree of correlation in a given system, the correlation factor $f_c = \kappa_{\text{FS}}/\kappa_{\text{MSD}} = \sum_{ij} \mathcal{C}_{ij} / \sum_i \mathcal{C}_{ii}$ is introduced as the ratio of the FS to MSD estimate of conductivity (it is the inverse of the Haven ratio).

Now we outline the spectral denoising approach to reduce the noise in the calculation of correlated ionic conductivity. (1) Diagonalize $\langle \mathcal{C}_{ij}(\tau_1) \rangle$, and obtain its eigenbasis \mathcal{A} . As $\langle \mathcal{C}_{ij}(\tau_1) \rangle$ is positive-definite and symmetric, it is always possible to find a complete set of real, orthonormal eigenvectors, and its eigenvalues are positive. (2) Rotate using \mathcal{A} all $\langle \mathcal{C}_{ij}(\tau_n) \rangle$, where $\tau_n > \tau_1$, obtaining $\Gamma(\tau_n) = \mathcal{A}^T \langle \mathcal{C}_{ij}(\tau_n) \rangle \mathcal{A}$. As we assume the system is in equilibrium and the correlation profile is stationary, we expect $\Gamma(\tau_n)$ to be nearly diagonal, with noise in the off-diagonal terms only arising from finite sampling of the time-window averages. This noise is confirmed numerically to have zero expectation value, as discussed in Section 4 of the Supplemental Material[20]. (3) Set to zero the off-diagonal terms of $\Gamma(\tau_n)$ obtaining $\Gamma^*(\tau_n)$, in the same spirit as in the Nernst-Einstein. The key difference is that we do this in the basis of natural diffusion eigenmodes identified from the covariance matrix of the system itself. (4) Rotate back $\Gamma^*(\tau_n)$ using the eigenbasis \mathcal{A} to obtain the denoised covariance matrix $\langle \mathcal{C}_{ij}^*(\tau_n) \rangle$ to then use in Equation 1. In addition to helping reduce the conductivity variance, the eigenbasis \mathcal{A} also provides a microscopic understanding of the fundamental modes of diffusion in correlated scenarios, as discussed below. The details regarding the choice of the optimal τ_1 , as well as the mathematical robustness of this approach are thoroughly discussed in Section 3 of the Supplemental Material[20]. We can prove that the SD method always outperforms the FS method if the eigenbasis \mathcal{A} is ideal, i.e. obtained from the true covariance matrix obtained with infinite statistics of the diffusion process. Specifically, in this limit the SD approach yields unbiased results, while the estimate variance is always strictly lower

than that of FS:

$$\begin{aligned} \text{Var} \left(\sum_{ij} \mathcal{C}_{ij}^* \right) &= 2 \sum_i (\lambda_i w_i^2)^2 \\ &\leq 2 \left(\sum_i \lambda_i w_i^2 \right)^2 = \text{Var} \left(\sum_{ij} \mathcal{C}_{ij} \right). \end{aligned}$$

Where $\lambda_i \geq 0$ are the diagonal elements of the Γ matrix, and w_i is the sum of all elements of the i th eigenvector, i.e., column of \mathcal{A} . In practice, $\langle \mathcal{C}_{ij}(\tau_1) \rangle$ is a finite-sampling approximation to the ideal covariance matrix. In this case, we can also prove that the SD approach outperforms the FS - full details of the proofs and derivations are given in Section 3 of the Supplemental Material[20].

III. VALIDATION & APPLICATIONS

1. Multivariate Gaussian Random Walk

In order to establish the methodology in a controlled model setting, we sample a multivariate Gaussian distribution to obtain correlated random displacement vectors that mimic Brownian diffusion with exactly known correlation. As the clusters of particles are potentially mutable, the time-block averaged $\langle \mathcal{C}_{ij}(\tau_1) \rangle$ contains the correlation information uniformly averaged over the blocks of off-diagonal terms corresponding to the same species-species correlations. More details are provided in Section 1 of the Supplemental Material[20]. Thus, we consider a model with the covariance matrix with $\mathcal{C}_{i=j} = \alpha$ and $\mathcal{C}_{i \neq j} = \beta$ that represents a homogeneous single-component system. A time series of n Brownian steps is then constructed by adding n sampled vectors, and our goal is to estimate the slope $D = \frac{\partial}{\partial \tau} \sum_{ij} \langle \mathcal{C}_{ij}(\tau) \rangle$ from the sampled displacement trajectories. By modifying the covariance matrix, we can test the applicability and robustness of our approach on a wide range of types and strengths of correlations. More details on the Gaussian sampling are discussed in Section 2 of the Supplemental Material[20].

For our testing, we set the number of Brownian steps to 1000, and a minimum of 10 averaged position-position correlation matrices $\langle \mathcal{C}_{ij}(\tau_n) \rangle$ to perform linear regression to obtain the slope D . The number N of simulated Brownian walkers, representing diffusing particles, ranges from 3 to 500. We study f_c in the range of 0.25 to 2.75. A system with $f_c = 1$ possesses no correlation (the sum of the off-diagonal covariance elements equals 0), while $f_c > 1$ and $0 < f_c < 1$ corresponds to systems with negative and positive overall correlation, respectively. For every (f_c, N) combination, we perform 100 independent simulations of the Brownian walkers.

Figure 1 shows two ways the SD approximation can be used to improve the determination of correlated transport properties with respect to the exact theory. Panel

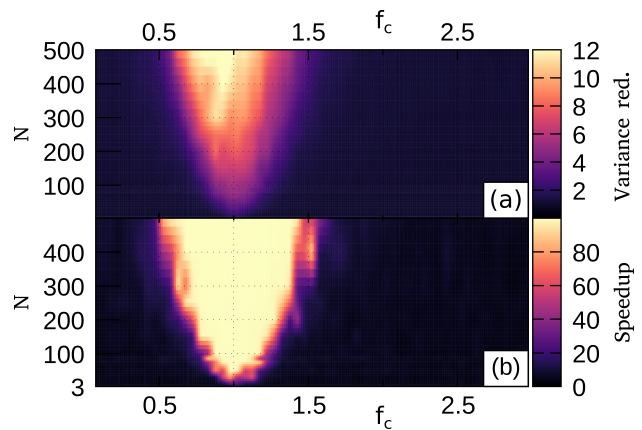


FIG. 1. Improvement of the SD estimates of the slope D of the multivariate Gaussian walk model: (a), the variance reduction and, (b), the computational speedup of the SD method, relative to the FS method.

(a) presents the reduction in the variance of the D estimate, calculated as the ratio between the regression variance of the FS and that of the SD approach. Panel (b) shows the computational speedup, calculated as the ratio $\frac{M_{\text{FS}}}{M_{\text{SD}}}$ of the number of Brownian steps required to achieve a given uncertainty by each method. We chose $M_{\text{FS}} = 1000$, thus the above expression conceptually reduces to how fast the SD method reaches the same accuracy as FS when 100% of the trajectory is used for the latter.

We make the following observations for this homogeneous single-component model example. (i) The off-diagonal elements of $\Gamma(\tau_n)$ that are set to zero are in fact distributed with a zero mean, confirming that they can be regarded as noise (see Section 4 of the Supplemental Material[20]). This numerically confirms our theoretical proof that the SD method is unbiased. (ii) Panels (a) and (b) show that the SD method produces more significant improvement in the weak-to-moderate correlation regimes, $0.5 < f_c < 1.5$. For strongly correlated single-component systems, the SD approach does not provide a considerable advantage over the FS method. Physically, in the latter regimes fluctuations of the ionic flux comprise the whole system, thus the total center of mass displacement of the system should be used to compute transport properties. (iii) The advantage of the SD method over the FS grows for larger system sizes. This is because the fluctuations of the center of mass decrease for larger systems, increasing estimate variance and thus requiring longer trajectories to converge. (iv) Crucially, the SD method *always* outperforms the FS method, as, for both the variance reduction and speedup, the values never fall below 1. Rigorous justification of this point, and derivations of the proofs of variance reduction are given in Section 3 of the Supplemental Material[20]. The last observation implies that the SD approximation can be applied to any system without prior assumptions on the correlation structure.

2. Lennard-Jones Liquid

We illustrate our approach by first studying the physical meaning of the eigenvectors of $\langle C_{ij}(\tau_1) \rangle$, and then by calculating D for a Lennard-Jones (LJ) interacting molecular system. We perform molecular dynamics (MD) simulations to generate atomic trajectories of two model systems: 1. one dimer and one trimer immersed in a bath of 500 monomers, and 2. 100 dimers in a bath of 15 000 monomers. For both systems, the intra-molecular interactions, or bonds, are modeled with simple harmonic springs, while the inter-molecular interactions are governed by a 12-6 LJ potential. We adopt LJ reduced units, and an appropriate rescaling renders all physical quantities dimensionless[21], thus we omit indicating the units. A timestep $\delta t = 10^{-3}$ is used to evolve the equation of motions via the velocity-Verlet integration algorithm. Once thermalized in the isothermal-isobaric ensemble for $6 \times 10^6 \delta t$ (Section 6 of the Supplemental Material[20]), the position of the particles of interest (those constituting the dimers and trimer) are recorded every $1 k\delta t$ over a $5 \times 10^4 k\delta t$ simulation of the canonical ensemble.

The study of the meaning of the eigenvectors of $\langle C_{ij}(\tau_1) \rangle$ is presented in panels (a-c) of Figure 2. Panel

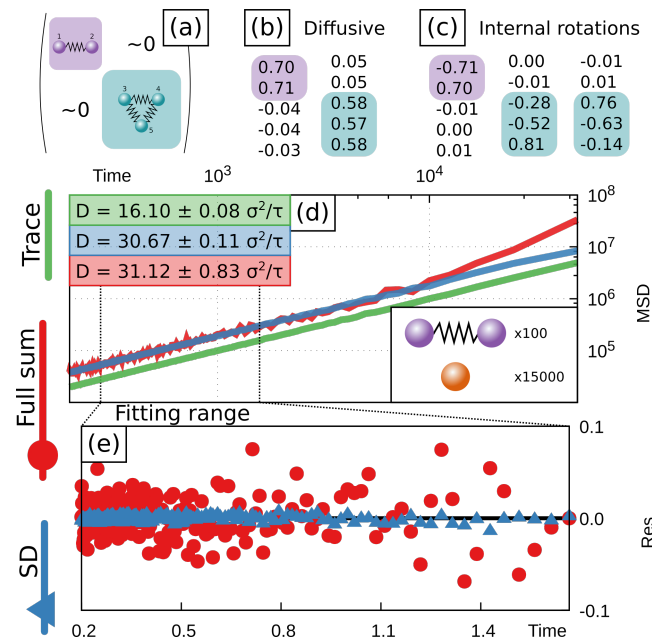


FIG. 2. Lennard-Jones liquid diffusion results. (a) structure of $\langle C_{ij}(\tau_1) \rangle$ for a single dimer and trimer in a bath of monomers; (b) and (c) covariance matrix eigenvectors; (d) time evolution of $\sum_{ij} \langle C_{ij}(\tau) \rangle$ for a system of 100 dimers in a bath of monomers, calculated with: uncorrelated trace method (green), full correlation sum (red), and the SD approach (blue); (e) residuals of the linear fit to compute the diffusion constant for the dimers in (d).

(a) represents the structure of $\langle C_{ij}(\tau_1) \rangle$, consisting of

three components: the diagonal, the inter-species off-diagonal, and the intra-species off-diagonal entries. Each entry on the diagonal is the single-particle mean-squared displacement after time τ_1 . In this dilute case the inter-species off-diagonal entries of (a) converge to zero. On the contrary, the bonded atoms constituting the dimer and trimer have strong immutable correlation as they are bound to move together. As a result, $\langle C_{ij}(\tau_1) \rangle$ has the structure of a block diagonal matrix, as sketched in Figure 2(a).

Correspondingly, the eigenvectors of $\langle C_{ij}(\tau_1) \rangle$ are partitioned into two sets. One set corresponding to the diffusive drift of the center of mass of each molecule (b), and another set corresponding to non-diffusive intra-molecular motions, rotations and vibrations (c). Specifically, for the dimer (in Figure 2(a-c) highlighted in purple), there are two eigenvectors. The first eigenvector, approaching $(\frac{1}{\sqrt{2}}, \frac{1}{\sqrt{2}}, 0, 0, 0)$, indicates that two of the particles are part of a diffusive duplet, while the second $(-\frac{1}{\sqrt{2}}, \frac{1}{\sqrt{2}}, 0, 0, 0)$, corresponds to internal motion that does not contribute to diffusion and has vanishing eigenvalue in the limit of infinite statistics. In general, any eigenvector whose eigenvalue and vector components sum approach zero does not contribute to diffusion. Thus, eigenvectors of $\langle C_{ij}(\tau_1) \rangle$ have intuitive physical interpretation as collective diffusion modes of the system, and form an appropriate basis for analysing diffusive transport. This method thus provides an unsupervised automatic way to identify diffusing clusters and molecules in the case of strong short-range correlations, from only atomic motion without any prior information.

Figure 2(d,e) show our approach applied to the calculation of D of a dilute solution of dimers in a bath of monomers. The top panel shows $\sum_{ij} \langle C_{ij}(\tau) \rangle$ over time for three approaches: trace (green), FS (red), and SD (blue). Due to weak inter-dimer and strong intra-dimer correlation, as the uncorrelated trace method applied to individual atoms, neglecting the $i \neq j$ entries would underestimate D by a factor of two. Indeed we compute the trace D_{MSD} to be 48% of the correlated D_{SD} . Panel (e) shows the residuals of the fitting used to compute D ; red circles for the FS, blue triangles for the SD method. Over the same time interval, the residuals of the SD method are considerably smaller than the residuals of the FS approach. Consequently, with the same amount of data, the SD method yields unbiased D as compared to the true FS correlated value, but with standard deviation 80% lower than that of the FS approach.

3. Electrolyte Conductivity

As a realistic test of our method, we calculate the conductivity κ for two battery electrolyte systems: 1. a lithium salt $\text{Li}^+[\text{TFO}]^-$ in an ionic liquid (IL), $[\text{Emim}]^+[\text{TFO}]^-$, and 2. an amorphous lithium phosphate ceramic, Li_3PO_4 . These systems have been

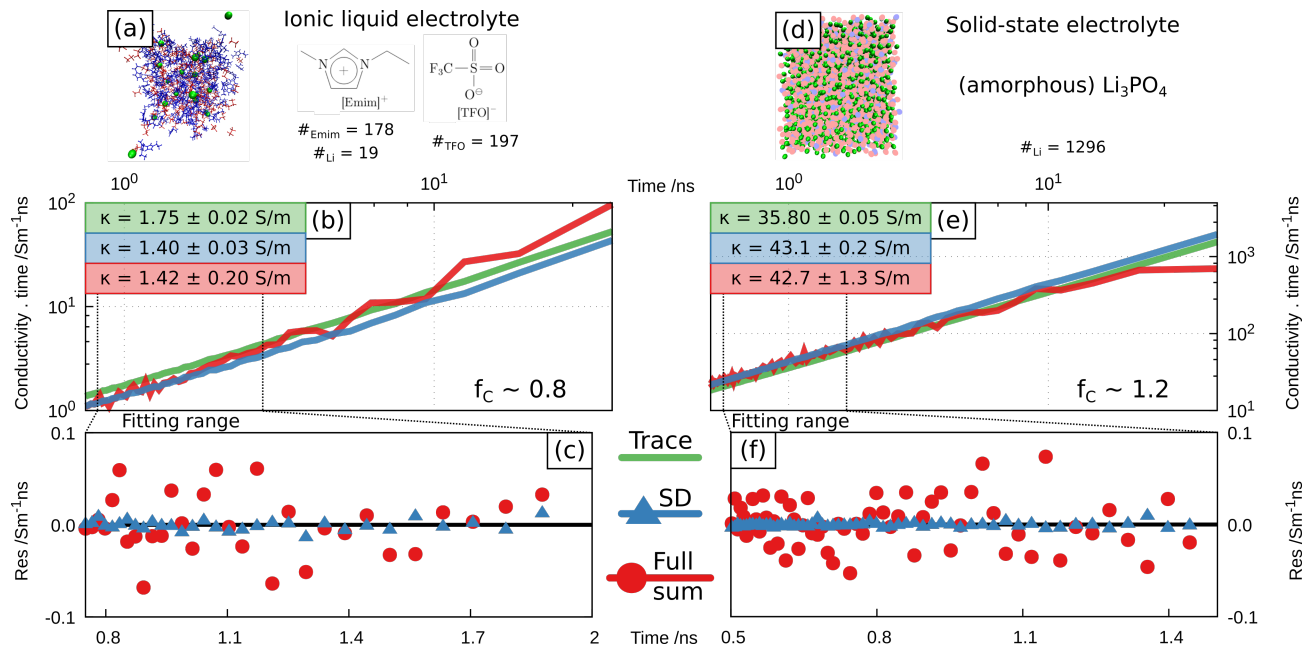


FIG. 3. SD method applied to the calculation of κ for two electrolyte systems: $\text{Li}^+[\text{TFO}]^-$ in $[\text{Emim}]^+[\text{TFO}]^-$ ionic liquid (a-c), and amorphous Li_3PO_4 (d-f). (a) and (d) show snapshots of the structures, and the number of charged mobile species. (b) and (e) show $\sum_{ij} \langle \mathcal{C}_{ij}(\tau) \rangle$ as computed with the three different methods. Finally, (c) and (f) show the residuals over the time range used to compute κ .

shown to exhibit significant ion-ion correlation both theoretically[9, 11, 22] and experimentally[12, 23, 24], with f_c from 0.6 to as high as 5. The computed f_c are 0.8 and 1.2 for the ionic liquid-based and solid state electrolyte, respectively. Consequently, if the MSD method is used on these systems, it would result in a 20% overestimation and underestimation, respectively.

We perform MD simulations and analyze the atomic displacement correlations to compute κ with the three methods: trace, FS, and SD. The ionic liquid-based electrolyte is composed of 178 1-Ethyl-3-methylimidazolium ($[\text{Emim}]^+$), 19 Li^+ , and 197 trifluoromethanesulfonate ($[\text{TFO}]^-$) molecules, leading to a Li^+ -salt molar fraction of 0.1, Figure 3(a). The interatomic potentials, the structure generation and equilibration protocols are inherited from our previous works[8, 11, 25]. For Li_3PO_4 , we create a supercell of the crystalline structure comprising a total of 3456 atoms, 1296 of which are Li^+ ; the force-field parameters are taken from an existing library [26]. Full details can be found in Section 6 of the Supplemental Material[20].

Panels (b) and (e) show the drift over time of $\sum_{ij} \langle \mathcal{C}_{ij}(\tau) \rangle$ for the trace (green), FS (red), and SD (blue) approaches. As in the other models discussed above, Figure 2, the displacement correlation $\sum_{ij} \langle \mathcal{C}_{ij}(\tau) \rangle$ is significantly less noisy for the SD method compared to the FS approach, and this translates to lower residuals, Figure 3(c,f) for both systems, with κ matching the FS values. The uncertainty of the κ estimate is reduced by $\sim 70\%$ for both electrolyte systems.

IV. CONCLUSIONS

In summary, we provide a superior approach capable of reducing the uncertainty of conductivity estimates of correlated systems. This is achieved by leveraging the correlation information encoded in the well-converged short-time position-position covariance matrix. The spectral analysis of the position-position covariance matrix is shown to be an unsupervised way to uncover stable collective diffusion modes and particle clusters, automatically revealing the microscopic physical mechanisms underpinning ionic transport in complex systems, without prior information as required for previously available methods. Consequently, it enables accurate estimates of transport properties from significantly shorter molecular dynamics trajectories, by several orders of magnitude for larger systems, while capturing the full correlation contribution of the total flux, exact full summation approach. We derive formal justification that the results are unbiased and provide rigorous bounds on the reduction of the variance of the estimates. In addition, we numerically demonstrate the improvement and applicability of our approach on controlled models and two realistic electrolyte systems: $\text{Li}^+[\text{TFO}]^-$ in $[\text{Emim}]^+[\text{TFO}]^-$ ionic liquid-based and Li_3PO_4 solid-state battery electrolytes. These results open the possibility of rapid investigation of transport characteristics in complex concentrated electrolytes where correlation effects cannot be neglected.

We acknowledge useful discussions with Eric R. Fadel.

-
- [1] J. B. Goodenough, Reports on Progress in Physics **67**, 1915 (2004).
- [2] A. Fuliński, Physical review letters **79**, 4926 (1997).
- [3] J. C. Bachman, S. Muy, A. Grimaud, H.-H. Chang, N. Pour, S. F. Lux, O. Paschos, F. Maglia, S. Lupart, P. Lamp, *et al.*, Chemical reviews **116**, 140 (2016).
- [4] R. Schmuch, R. Wagner, G. Hörpel, T. Placke, and M. Winter, Nature Energy **3**, 267 (2018).
- [5] K. Xu, Chemical reviews **114**, 11503 (2014).
- [6] A. Balducci and P. Gerlach, ChemElectroChem.
- [7] B. Qiao, G. M. Leverick, W. Zhao, A. H. Flood, J. A. Johnson, and Y. Shao-Horn, Journal of the American Chemical Society **140**, 10932 (2018).
- [8] N. Molinari, J. P. Mailoa, N. Craig, J. Christensen, and B. Kozinsky, Journal of Power Sources **428**, 27 (2019).
- [9] X. He, Y. Zhu, and Y. Mo, Nature communications **8**, 15893 (2017).
- [10] G. Murch, Solid State Ionics **7**, 177 (1982).
- [11] N. Molinari, J. P. Mailoa, and B. Kozinsky, The journal of physical chemistry letters (2019).
- [12] M. Gouverneur, F. Schmidt, and M. Schönhoff, Physical Chemistry Chemical Physics **20**, 7470 (2018).
- [13] D. R. Wheeler and J. Newman, The Journal of Physical Chemistry B **108**, 18353 (2004).
- [14] D. R. Wheeler and J. Newman, The Journal of Physical Chemistry B **108**, 18362 (2004).
- [15] A. France-Lanord and J. C. Grossman, Physical review letters **122**, 136001 (2019).
- [16] R. Kubo, Journal of the Physical Society of Japan **12**, 570 (1957).
- [17] N. F. Mott and R. W. Gurney, (1940).
- [18] F. Müller-Plathe and W. F. van Gunsteren, The Journal of chemical physics **103**, 4745 (1995).
- [19] M. P. Allen and D. J. Tildesley, *Computer simulation of liquids* (Oxford university press, 2017).
- [20] N. Molinari, Y. Xie, I. Leifer, and B. Kozinsky, Supplemental material.
- [21] D. Frenkel and B. Smit, *Understanding molecular simulation: from algorithms to applications*, Vol. 1 (Elsevier, 2001).
- [22] A. Marcolongo and N. Marzari, Physical Review Materials **1**, 025402 (2017).
- [23] N. Kuwata, X. Lu, T. Miyazaki, Y. Iwai, T. Tanabe, and J. Kawamura, Solid State Ionics **294**, 59 (2016).
- [24] M. P. Rosenwinkel and M. Schönhoff, Journal of The Electrochemical Society **166**, A1977 (2019).
- [25] E. R. Fadel, F. Faglioni, G. Samsonidze, N. Molinari, B. V. Merinov, W. A. Goddard III, J. C. Grossman, J. P. Mailoa, and B. Kozinsky, Nature communications **10**, 1 (2019).
- [26] A. Pedone, G. Malavasi, M. C. Menziani, A. N. Cormack, and U. Segre, The Journal of Physical Chemistry B **110**, 11780 (2006).